G.N. Sankin[1], R. Mettin[2], W. Lauterborn[2], V.S. Teslenko[1]

SECONDARY ACOUSTIC WAVES IN SHOCK INDUCED CAVITATION BUBBLE CLOUDS

[1]Lavrentyev Institute of Hydrodynamics of SB RAS,
pr. ac. Lavrentieva, 15, 630090 Novosibirsk, Russia
Phone: +7-3832-333047; Fax: +7-3832-331612
E-mail: sankin@hydro.nsc.ru
[2]Drittes Physikalisches Institut, Universität Göttingen
Bürgerstraße 42-44, 37073 Göttingen, Germany

Bubble cloud dynamics and acoustic waves at cavitation after a focused shock wave are investigated experimentally by high-speed photo-recording and fiber-optic hydrophone measurements. Secondary acoustic waves from finite cavitational clouds far from boundaries and near to the free surface are observed. The correlation between secondary acoustic cavitation waves and luminescence at an early stage of cavitation is discussed.

INTRODUCTION

Bubble dynamics is a key point for mechanisms of interaction between converging shock waves and medium in lithotriptor devices. When bubbles collapse violently they emit a shock wave with an amplitude possibly exeeding the pressure in the primary wave [1]. High temperatures and velocity shear in bubble clouds are known to be additional effect of shock waves in liquids [2].

Numerous attempts have been made to calculate the pressure in a liquid from a convergent acoustic pulse [3] and from collapsing bubbles [4]. An effect which follows from the Gilmore-Akulichev model for bubble dynamics and pressure wave emission is a relaxation (unloading) wave [5]. In the negative pressure phase of a short high acoustic pulse and if one can neglect the gas diffusion into the bubble [6], the internal pressure is insignificant, and the pressure at the expanding bubble wall is zero. Taking into account the fast expansion speed of bubbles of different size, it means a rapid relaxation of the negative pressure to zero for the primary acoustic pulse. During the non-linear propagation the transformation of the relaxation wave even to a positive pressure peak is possible to observe in the theory [5] and in the experiment [7].

The mechanism described dramatically influences the propagation of convergent or reflected acoustic pulses in a liquid. In this paper some experimental results on the generation of such secondary cavitation waves (SCW) and their role for luminescence are presented.

EXPERIMENTAL SETUP

An electromagnetic generator for focused shock waves, manufactured at the Lavrentyev Institute of Hydrodynamics of the Siberian Division of the Russian Academy of Sciences in Novosibirsk, is used. The tranducer based on the principle from [8] has an aperture of D = 70 mm, and the curvature radius of 55 mm determines the focal distance F = 55 mm. A low inductance capacitor C of 1 μF or 2 μF is discharged through a coil to generate a high pulse current. A membrane on the coil is pushed off, and an acoustic pulse is generated in the liquid. The pressure amplitude of the initial pulse can be controlled via the generator voltage U_g from 5 to 10 kV on the capacity found to be proportional to the amplitude of the current in the coil. The rise time of the current amounts to 0.5 μs (for C = 2 μF, from 10% to 90% I_{max}) and is independent of the voltage. During propagation to the focus the acoustic pulse is transformed under certain conditions into a shock.

The tranduser is installed at the bottom of a cubic Kaprolon (kind of polyamide) cuvette. The walls of the cuvette contain spherical glass windows, which allow observation and illumination of the focal area. We used distilled, demineralized water saturated with gas in room atmosphere.

Pressure disturbance measurements were done with a fiber optic hydrophone (FOPH 300, [9]). To observe shock wave propagation and bubble dynamics a high-speed camera (IMACON 468, DRS Hadland, 8 frames, 10 ns exposure time) was used. A sufficient magnification of up to 3 μm per pixel was achieved with optic lenses (Nikon). The light emission was recorded by a PMT (Hamamatsu R5600U-06, spectral range from 260 to 530 nm, 2 ns rise and 3.8 ns fall time). For the purpose of space and time resolution, the focal area of the cuvette was focused in scale 1:0.9 on a quadratic diaphragm (side length $\delta = 1.2$ mm) by a 50 mm objective (Nikon). Hence, the timing uncertainty between shock wave and light was limited to $1.1 \cdot \delta / c_0 = 0.9$ μs, where $c_0 = 1.5$ mm/μs is the sound speed in water. The signal was recorded using a fast digital sampling oscilloscope (TDS 784A, Tektronix, 1 GHz analog bandwith, 4 GS/s sampling rate, 8 bit).

RESULTS AND DISCUSSION

Pressure history. In Fig.1 the general picture of cavitation phenomena is presented. In this experiment the shock was launched from below and the liquid surface at the top of the frames was in the focal plane of the transducer. The first cavitation cloud (4) is produced by the primary wave (1-2) and is elongated (cigar shaped) with the center situated about 10 mm below focus. The second cloud (6) of very small bubbles with the shape of a (probably hollow) cap looks fog-like and is produced by the superposition of the reflected wave (7) and primary rarefaction wave (between fronts 1 and 2) directly under the free surface. The top of the cap is broadened by a fog ring of bubbles (5).

During the propagation and reflection under cavitation a significant disturbance of the wave picture is observed. Secondary waves (2) and (3) are visible running from both cavitation clouds. The crossing of normals to the wave fronts of both (2) and (3) determine their sources within the cavitation clouds below the focal point. It is suggested that cavitation is the reason for the secondary waves. The spatial distance between waves (1) and (2) is measured both by high-speed photo-recording and by the fiber optic hydrophone as 3.9 mm. This distance can be recalculated using the speed of sound to the time 2.6 μs. Consequently a bubble collapses two times in peaks (1) and (2). The temporal interval between two positive pressure peaks and between light flashes is, hence, expected to be equal.

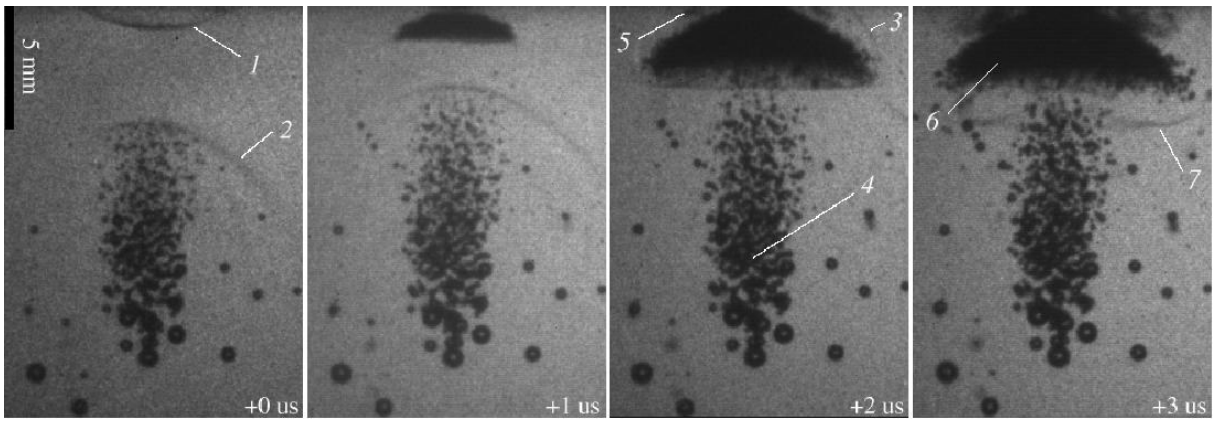

Fig.1. Shock-wave induced breakdown in water near a free surface (on top) for U_g = 9 kV. The numbers are described in the text.The timing and scale are given in the frames.

Figure 2 shows the detailed pressure history near the different cavitation bubble clouds. For cavitation far from boundaries the secondary wave (2) is detected at hydrophone positions from (a) to (d) in Fig.2,A. The results are shown for $U_g = 9$ kV and $C = 2$ μF when conditions are appropriate for extended cavitation. Both no secondary wave and significant bubble dynamics are found for 5 kV (pressure trace $b^{//}$ in Fig.2b) and 6 kV. The visible front (2) corresponds to a positive pressure gradient. Under certain conditions it is transformed into a shock wave and becomes contrastly observable with the given technique. It is important to note that there is almost no bubble in front of this secondary wave. Therefore we conjecture a generation mechanism due to cavitation, and we call it a secondary cavitation wave (SCW). Another indication is that the observed bubble volume is

increased by a factor of about 300 when the voltage U_g is changed from 5 kV (no SCW) to 9 kV (strongest SCW). The SCW is a peak on the pressure oscillogram with the front starting at the minimum of pressure. The duration of the SCW is less than the duration of the negative pulse of the primary wave, and the edge rarefraction wave continues after the SCW peak. This is in contrast to the theoretical calculation given in [3] and can be explained using a cavitational model for SCW origin.

The gas and vapor cavities can be distinguished from acoustic waves by the speed of propagation and the time of stability. The virtual velocity of the bottom of the cap-like bubble cloud is about two times higher than the speed of sound in water due to a geometrical effect. When the waves have left the frame, the bubble life time is determined by the usual (Rayleigh) collapse time for an effective radius of bubble cloud.

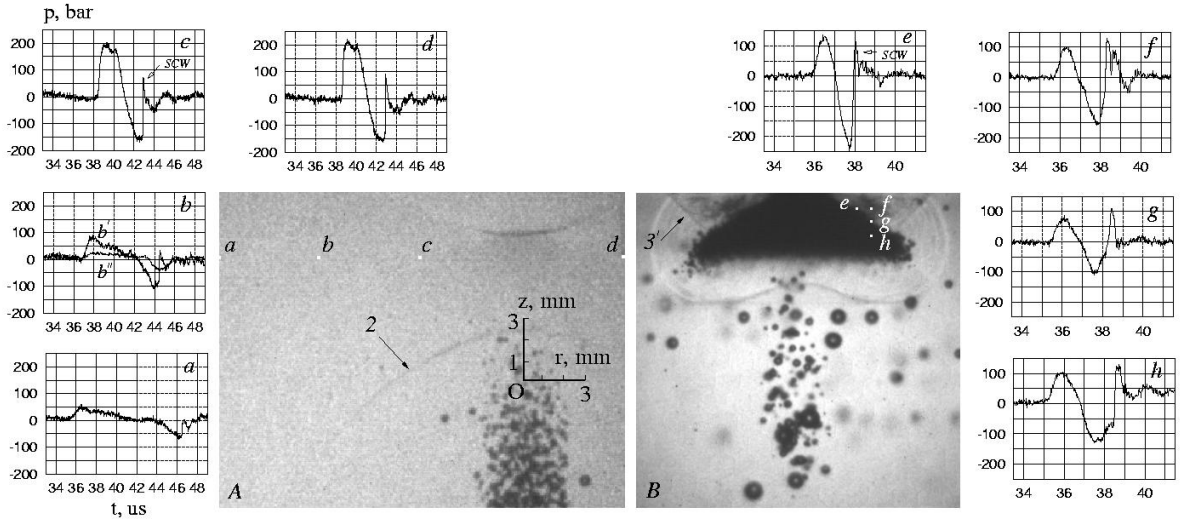

Fig.2. Pressure recording in water and hydrophone positions using axial coordinate system (r,z) with the origin at the focus and the units in mm. A: shock focus as indicated, C = 2 uF, U_g = 9 kV, t = 40 μs; oscillograms for C = 2 μF, U_g = 9 kV (b'' - C = 2 μF, U_g = 5 kV) for hydrophone positions: a = (-15,6), b = (-10,6), c = (-5,6), d = (5,6). B: shock focus on central top, C = 2 μF, U_g = 7 kV, t = 39 μs, oscillograms for C = 1 μF, U_g = 6 kV for hydrophone positions e = (2,-0.5), f = (2.5,-0.5), g = (2.5,-1), h = (2.5,-1.5).

The pressure data (e) to (h) are compared for C = 1 μF, U_g = 6 kV (hydrophone positions are shown in Fig.2,B). The given voltage provides no secondary waves in the bulk that can disturb the wave pattern observed near the free surface. The oscillograms show the primary compression pulse and following after that the rarefraction pulse in superposition with the reflected and inverted primary pulse. The wave pattern results in a wave radiated by the cavitation cloud. This wave undergoes a secondary reflection from the free surface inverting the pressure. The SCW parts before and after reflection interfere with each other on the vertical symmetry axis. It is found from the timing of the pressure recordings that a compression pulse is running from point (e) to (f) and from (f) to (h) with an angle between front and free surface of 65±5 degrees. It can be associated with the reflected wave ($3'$) in the Fig.2,B. Hence the restore wave pattern is in agreement with the waves observed with high-speed photo-recording.

Luminescence. Despite of that no separate bubbles can be resolved in the fog-like cloud near the free surface, it is possible to investigate the bubble dynamics in this cloud by luminescence registration.

In Fig.3 luminescence of the fog-like cloud is presented summarized for 16 shots. The generator worked in a fast shot regime with a repetition rate of 0.16 Hz, where bubbles from previous shots remain until the next shot with a number related to the negative peak pressure. The region observed by the PMT is directly below the focus at the free surface. The luminecsence is observed as three temporal groups of flashes. The quantitative values for pressure measurements and luminescence

for different voltages are displayed in Table 1. From time analysis of the oscillograms the time interval between the first and third group is found to be 1.7±0.4 μs which is close to the collision time of the secondary wave and the bottom of the cap cloud estimated from the wave pattern. The first and third group can be correlated to the positive and negative pressure peak (p_1^+, p_1^-) and the secondary positive pressure peak (p_2^+), respectively. The data in Table 1 have good correlation between peak pressures and flash luminosity, which supports an adiabatic collapse model for luminescence.

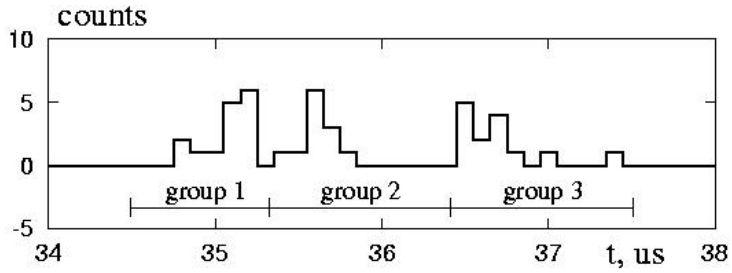

Fig.3. Histogram luminescence signal accumulated for 16 shots for U_g=8 kV in 10% glycerin in water.

Table 1. Amplitudes of pressures and luminescence; recording positions as indicated.

U_g, kV	p_1^+, bar z = 0 r = 0	p_1^-, bar z = 0 r = 0	p_2^+, bar z = 3 mm r = 5 mm	Luminescence, counts z = -0.6 mm, r = 0		
				group 1	group 2	group 3
5	650±50	-180±30	0±5	1	9	1
6	700±50	-200±30	10±5	8	18	4
7	750±50	-330±30	40±5	8	13	8
8	750±50	-390±30	60±5	15	12	14
9	750±50	-420±30	80±5	-	-	-

The possible reason for the second group is the secondary wave ($3^/$) reflected from the free surface (marked in Fig.2e as SCW) using the adiabatic collapse model. The detailed bubble dynamics in the fog-like cloud (6) under conditions of fast spreading cavitation still has to be revealed.

This work was supported by DAAD grant No. A/00/01480, grant No. 01-02-06444 from RFBR, and partially by grant No. 00-02-17992 from RFBR.

REFERENCES

1. Lindau O. and Lauterborn W., in: Nonlinear acoustics at the turn of the millennium. ISNA-15. Eds: W.Lauterborn, T.Kurz, AIP Conference Proceedings, 2000, v524, pp.385-388.
2. Crum L.A. Sonoluminescence, sonochemistry, and sonophysics. J. Acoust. Soc. Am., 1994, v95, N1, pp.559-562.
3. Coleman A.J., Choi M.J., and Saunders J.E. Theoretical prediction of the acoustic pressure generated by a shock wave lithotripter. Ultrasound in Medicine and Biology, 1991, v17, N3, pp.245-255.
4. Akulichev V.A., Boguslavskii Yu.Ya., Ioffe A.I., Naugol'nykh K.A. Radiation of finite-amplitude spherical waves. Soviet physics - Acoustics, 1968, v13, N3, pp.281-285.
5. Kedrinskii V.K. Hydrodynamics of explosions. J. Appl. Mech & Tech. Phys., 1987, v28, N4, pp.491-515.
6. Church C.C. A theoretical study of cavitation generated by an extracorporeal shock wave lithotripter. J. Acoust. Soc. Am., 1989, v86, N1, pp.215-227.
7. Teslenko V.S. Shock-wave breakdown in liquid. Kinetics of stimulated acoustic scattering at focusing of shock waves. Pis'ma v Zhurnal Tekhnicheskoi Fiziki, 1994, v20, pp.51-56 (in Russian).
8. Eisenmenger W. Elektromagnetische Erzeugung von ebenen Druckstößen in Flüssigkeiten. Acustica, 1962, v12, pp.185-202 (in German).
9. Staudenraus J. and Eisenmenger W. Fibre-optic probe hydrophone for ultrasonic and shock wave measurement in water. Ultrasonics, 1993, v31, pp.267-273.